Prediction of Critical Points: A New Methodology Using Global Optimization

Nélio Henderson, Léa Freitas, and Gustavo M. Platt
Thermodynamics and Optimization Group (TOG), Instituto Politécnico, Universidade do Estado do Rio de Janeiro, 28601-970, Nova Friburgo-RJ, Brazil

DOI 10.1002/aic.10119
Published online in Wiley InterScience (www.interscience.wiley.com).

*In the present work we develop, implement, and analyze the results of a new methodology destined to calculate critical points of phase transitions. Our criticality conditions are developed from a slight modification of the Gibbs tangent plane criterion. We formulate the critical points calculation as an optimization problem. Such formulation offers many advantages, among them we can mention the capability of determining more than one critical point, the use of robust numerical methods, and the possibility of visualization of the critical phenomenon from a two-variable (*T *and* P*) objective function. To solve the optimization problems we use the simulated annealing algorithm, a stochastic method whose convergence does not depend on initial guesses and gives preference to global optima. Several samples of mixtures were used to test the present methodology. The results of our simulations were compared, in a satisfactory way, with experimental data and with some results calculated in other approaches.* © 2004 American Institute of Chemical Engineers *AIChE J,* 50: 1300–1314, 2004
Keywords: Gibbs tangent plane criterion, global optimization, thermodynamic system, objective function, critical point

Introduction

A critical point of a thermodynamic system is reached when there is no longer any difference in the physical properties between coexisting phases. There are many important examples of high-pressure processes in chemical and petroleum engineering where critical point calculations are required. Indeed, the critical properties are necessary for adequate design of chemical reactors and separation equipment, processes involving supercritical fluid extraction, and in enhancement of oil-recovery techniques. The location of the critical point determines whether retrograde condensation will occur in compositional simulators, typically used in petroleum industry for simulated condensing gas drive and miscible gas injection. In tertiary recovery processes the location of critical point is also fundamental to predict regions of complete miscibility, where the resident fluid is dislocated by the injected gas. Thus, of course, calculations of the critical points are important in several processes involving fluid phase equilibria at high pressure. Besides, as discussed by Sadus (1994), the study of critical equilibrium is also of considerable practical utility in understanding the phase equilibrium of fluids in general. This author emphasizes that the critical state can be used to determine the global nature of the phase behavior of a mixture, according to the phase behavior classification of van Konynenburg and Scott (1980), for binary mixtures, based on critical transitions.

Gibbs (1928), in his fundamental work on the equilibrium of heterogeneous substances, was the first to establish thermodynamic criteria for the criticality conditions of fluid systems. The application of Gibbs critical criteria to the calculation of critical points of a multicomponent (with more than three components) mixture was first attempted by Peng and Robinson (1977). Several years before, Spear et al. (1971) had studied calculations of critical points in ternary mixtures. A revision on this subject is presented in Hicks and Young

Correspondence concerning this article should be addressed to N. Henderson at nelio@iprj.uerj.br.

(1975). Peng and Robinson (1977) was shown that the proposed equation of state was capable of generating reliable results for the critical condition. Hicks and Young (1977) presented an algorithm for location of critical points that works by monitoring the sign of the one critical condition, whereas searches to zero use the other one at the temperature–volume plane. Later, Baker and Luks (1980) used the Redlich–Kwong equation of state and the Gibbs criticality criteria based on Helmholtz free energy, as modified by Reid and Beegle (1977). These approaches require the evaluation of two determinants of order $r - 1$ for an r-component system. The evaluation of these determinants is a computationally expensive part of the Gibbs formulation, particularly for mixtures with many components. To minimize the complexity of the computational calculations, Heidemann and Khalil (1980) proposed equivalent forms of the criticality criteria that are based on the stability of homogeneous phases, defined in terms of a Taylor expansion of the Helmholtz energy. Their computation procedure avoids differentiation of determinants and requires, during each iteration, the evaluation of only one determinant, the evaluation of a set of linear simultaneous equations, and the evaluation of a triple summation function. To reduce still further the amount of computation, this procedure has been refined by other workers [see, for example, Billingsley and Lam (1986); Eaton (1988); Kolář and Kojima (1996); Michelsen (1980); Michelsen and Heidemann (1981)].

Criteria for critical points based on the expansion of the tangent plane distance function of Gibbs energy have been developed by Michelsen (1984). This function describes the thermodynamic stability criterion proposed originally by Gibbs (1928), proved by Baker et al. (1982), and first implemented by Michelsen (1982). The substantial difference in the conditions established by Michelsen (1984) resides in the fact of the temperature and pressure to be the primary variables, whereas Heidemann and Khalil used the pressure and volume. Michelsen (1984) also developed a new technique for direct computation of critical points that does not involve the evaluation of any determinants and uses eigenvalue methods. The critical temperature and pressure are determined by a Newton method and a deficiency of the Michelsen methodology is that rather close initial estimates are required.

More recently, Stradi et al. (2001) proposed a new numerical approach to resolve the nonlinear system that describes the Heidemann–Khalil formulation of the criticality conditions. The procedure used by Stradi and coworkers is based on interval analysis: an interval Newton/generalized bisection algorithm is used. This procedure is initialization-independent and the authors guarantee that all mixture critical points are located.

In the present work, we describe the formulation, implementation, and analysis of the results of a new methodology for the calculation of the critical points of multicomponent mixtures. Criticality criteria are found by expansion of a slight modification of the tangent plane distance function of Gibbs energy. This criterion is used to formulate, for the first time, the critical point calculation as an optimization problem. Such formulation offers many advantages, among which we can mention the capability of determining more than one critical point and the use of robust numerical methods. The formulation also allows visualization of the critical phenomenon from the analysis of the surface and of the contour curves of a two-variable (T and P) objective function, which helps to understand the complexity involved in the determination of critical points, showing the existence of several local minima (nor all global ones) located in regions difficult to access for classic methods of optimization. To find out the global minimum of this objective function, the simulated annealing (SA) algorithm version as formulated by Corana et al. (1987) was chosen. The SA is a stochastic method for obtaining good solutions to difficult optimization problems, which has received much attention over the last few years, whose convergence does not depend on initial guesses and gives preference to global optima.

Model Formulation

The Gibbs tangent plane criterion

Following the Gibbs tangent plane criterion analyzed by Baker et al. (1982) [also see Michelsen (1982) and Henderson et al. (2001)], we assume that in the presence of a small perturbation an r-component mixture with global molar composition $z = (z_1, z_2, \ldots, z_r)$ is divided in two phases, the original phase and a hypothetical phase. Denoting by x_i and μ_i, respectively, the molar fraction and the chemical potential for each component in hypothetical phase, we can write the stability condition in the usual form

$$d = \sum_{i=1}^{r} x_i[\mu_i(x_1, \ldots, x_r) - \mu_i^0] \geq 0 \qquad (1)$$

where $\mu_i^0 = \mu_i(z_1, \ldots, z_r)$ represents the chemical potential of the component i evaluated at the global composition $z = (z_1, z_2, \ldots, z_r)$. If n is total number of moles in the hypothetical phase and G is the Gibbs energy associated, then d can be written in the form $d = g - \tau$, where

$$g = \frac{G}{n} = \sum_{i=1}^{r} x_i\mu_i(x_i, \ldots, x_r)$$

is the molar Gibbs energy of the hypothetical phase and $\tau = \sum_{i=1}^{r} x_i\mu_i^0$ is the function that represents the tangent plane to the surface g at the point $[z, g(z)]$. Thus, the tangent plane distance function for an r-component system can be geometrically defined as the vertical distance from the tangent plane to the surface of the molar Gibbs energy at global composition $z = (z_1, z_2, \ldots, z_r)$ to the surface itself at composition $x = (x_1, x_2, \ldots, x_r)$ relative the hypothetical phase.

The stability condition $d(x) = g(x) - \tau(x) \geq 0$, for all $0 < x_i < 1$ and $\sum_{i=1}^{r} x_i = 1$, implies that the molar Gibbs energy surface of the hypothetical phase (g) always lies above the tangent plane (τ) that passes through the point $[z, g(z)]$ [see Figure 1(a)]. If the mixture is unstable, then part of the surface of g is below the tangent plane τ, as shown in Figure 1(b).

Because of the geometric aspects described above, the stability condition given by Eq. 1 is known as Gibbs tangent plane criterion. The function d is called tangent plane distance function. This function is also designated stability test function because by using d it is possible to build methodologies, essentially numerical procedures, appropriate to test the stability of phases.

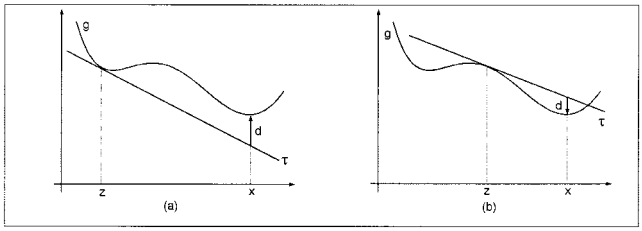

Figure 1. Tangent plane distance: (a) positive distance (stable); (b) negative distance (unstable).

The modified stability test function

To develop the criticality conditions used in this work, we modified slightly the stability test function. Other different modifications can be found in Nagarajan et al. (1991) and Henderson et al. (2001).

By substituting the constraint $x_r = 1 - \sum_{i=1}^{r-1} x_i$ into Eq. 1, the necessary and sufficient conditions for stability of an r-component mixture become

$$d(x) = \sum_{i=1}^{r-1} x_i\{[\mu_i(x) - \mu_i^0(z)] - [\mu_r(x) - \mu_r^0(z)]\} + [\mu_r(x) - \mu_r^0(z)] \geq 0 \quad (2)$$

for all $x = (x_1, \ldots, x_{r-1}) \in \Omega \subset R^{r-1}$, where $\mu_i(x) : \Omega \subset R^{r-1} \rightarrow R$ indicates that each chemical potential is defined in $\Omega = \{x \in R^{r-1}; 0 < x_i < 1, i = 1, \ldots, r-1, \text{ and } \sum_{i=1}^{r-1} x_i < 1\}$, the set of independent variables of the hypothetical phase.

Criticality criteria

Expanding the function $d(x)$ in the Taylor series around $z = (z_1, \ldots, z_{r-1}) \in \Omega$ in the direction of a nonnull vector $h \in R^{r-1}$, such that $z + h \in \Omega$, we obtain

$$d(z + h) = d(z) + \nabla d(z) \cdot h + \frac{1}{2} \nabla^2 d(z) \cdot h^2 + \frac{1}{6} \nabla^3 d(z) \cdot h^3 + o(\|h\|^4) \quad (3)$$

where

$$\nabla d(z) \cdot h = \sum_{i=1}^{r-1} \frac{\partial d(z)}{\partial x_i} h_i \qquad \nabla^2 d(z) \cdot h^2 = \sum_{i,j=1}^{r-1} \frac{\partial^2 d(z)}{\partial x_i \partial x_j} h_i h_j$$

and

$$\nabla^3 d(z) \cdot h^3 = \sum_{i,j,k=1}^{r-1} \frac{\partial^3 d(z)}{\partial x_i \partial x_j \partial x_k} h_i h_j h_k$$

The mathematical objects ∇d, $\nabla^2 d$, and $\nabla^3 d$ are, respectively, the first, second, and third order tensors of the derivatives of d.

The classical Gibbs–Duhem relation in the intensive variables [see Callen (1985)], at constant temperature and pressure, given by

$$\sum_{i=1}^{r} x_i d\mu_i(x) = 0 \quad (4)$$

guarantees that the determination of the first-order partial derivatives of $d(x)$ do not involve the calculation of the partial derivatives of $\mu_i(x)$. This useful result is summarized in the following proposition.

Proposition 1: The first-order tensor $\nabla d(x) = [\partial d(x)/\partial x_j] \in R^{r-1}$ [the gradient vector of $d(x)$] is determined, for all $j = 1, \ldots, r-1$ by relation

$$\frac{\partial d(x)}{\partial x_j} = [\mu_j(x) - \mu_j^0] - [\mu_r(x) - \mu_r^0] \quad (5)$$

Proof of Proposition 1 (*see Appendix A*)

Equations 2 and 5 show that $d(z) = 0$ and $\nabla d(z) = 0$. Thus, Eq. 3 can be rewritten in the following equivalent form

$$d(z + h) = \frac{1}{2} \nabla^2 d(z) \cdot h^2 + \frac{1}{6} \nabla^3 d(z) \cdot h^3 + o(\|h\|^4) \quad (6)$$

Taking $h = su$, where $u \in R^{r-1}$ is such that $u \cdot u = 1$ and $s \in R$, Eq. 6 becomes

$$d(z + h) = qs^2 + cs^3 + o(s^4) \quad (7)$$

where

$$q = \frac{1}{2} \nabla^2 d(z) \cdot u^2 \qquad \text{and} \qquad c = \frac{1}{6} \nabla^3 d(z) \cdot u^3 \quad (8)$$

Equation 7 shows that for all $h = su \in R^{r-1}$, with $|s|$ sufficiently small, the Taylor expansion is dominated by the quadratic form $q = (1/2)\nabla^2 d(z) \cdot u^2$, with $u \cdot u = 1$. Therefore, a necessary condition for the stability is given by

$$q = \frac{1}{2} \nabla^2 d(z) \cdot u^2 \geq 0 \quad (9)$$

If q is negative, then the mixture is intrinsically unstable. If q equals zero, then the mixture is at the limit of intrinsic stability [see Michelsen (1984)].

Given a global composition z, we defined the temperature and pressure at a critical point (z, T, P) as being a pair (T, P) where the mixture is stable, but it is at limit of intrinsic stability; that is, $d(x, T, P) \geq 0$, for all $x \in \Omega$, and $q(z, T, P) = 0$. Thus, from Eq. 7, at a critical point must occur $d(z + h, T, P) = cs^3 + o(s^4) \geq 0$, for all $h = su \in R^{r-1}$ with $z + h \in \Omega$, where now c becomes the dominant term. For this to be possible, without depending of the sign of cs^3 (which can vary with the choice of s), it is also necessary that at a critical point

happens $c(z, T, P) = 0$. Therefore, this definition can be restated as follows:

Definition: A pair (T, P) at a critical point of an r-component mixture, with global composition characterized by $z = (z_1, \ldots, z_{r-1})$ is defined by values of temperature and pressure for which exists a vector $u \in R^{r-1}$, with $u \cdot u = 1$, such that

$$q(z, T, P) = \frac{1}{2} \nabla^2 d(z) \cdot u^2 = 0 \tag{10a}$$

and

$$c(z, T, P) = \frac{1}{6} \nabla^3 d(z) \cdot u^3 = 0 \tag{11a}$$

Besides, at a critical point the mixture should be globally stable, that is,

$$d(x, T, P) \geq 0 \qquad \text{for all } x = (x_1, \ldots, x_{r-1}) \in \Omega \tag{12}$$

Sometimes one deals in the practice with binary mixtures. Given that in the present work $\nabla^2 d(z) \in R^{(r-1)\times(r-1)}$ and $\nabla^3 d(z) \in R^{(r-1)\times(r-1)\times(r-1)}$, it follows from our formulation that in cases where $r = 2$ these tensors become scalars

$$\nabla^2 d(z) \equiv \frac{\partial^2 d(z)}{\partial x_1^2} \qquad \text{and} \qquad \nabla^3 d(z) \equiv \frac{\partial^3 d(z)}{\partial x_1^3}$$

u becomes essentially 1 and the criticality criteria, Eqs. 10a and 11a, take the simple forms

$$q(z, T, P) = \frac{1}{2} \frac{\partial^2 d(z, T, P)}{\partial x_1^2} = 0 \tag{10b}$$

$$c(z, T, P) = \frac{1}{6} \frac{\partial^3 d(z, T, P)}{\partial x_1^3} = 0 \tag{11b}$$

In procedures used in critical points calculation, as proposed by Heidemann and Khalil (1980), the stability condition, Eq. 12, which guarantees the stability of the critical point, is considered a test to be accomplished after the determination of T and P.

The classical critical conditions [see, e.g., Tester and Modell (1997)], in terms of the derivatives of Gibbs free energy, affirm that in a critical point, for a binary mixture, the second and the third derivatives Gibbs free energy, with respect to composition, must be equal to zero and a derivative of higher order must be greater than zero. The following proposition, relative to binary mixtures, demonstrates that the critical conditions given by Eqs. 10, 11, and 12 are entirely equivalent to the classic conditions cited above.

Proposition 2: For a binary mixture with global composition z_1 (and $z_2 = 1 - z_1$), a pair (T, P) satisfies the relationships

$$\frac{\partial^2 d(z_1, T, P)}{\partial x_1^2} = 0 \qquad \frac{\partial^3 d(z_1, T, P)}{\partial x_1^3} = 0$$

and $d(x_1, T, P) \geq 0$ for all $0 < x_1 < 1$; if, and only if,

$$\frac{\partial^2 g(z_1, T, P)}{\partial x_1^2} = 0 \qquad \frac{\partial^3 g(z_1, T, P)}{\partial x_1^3} = 0$$

$$\text{and} \qquad \frac{\partial^k g(z_1, T, P)}{\partial x_1^k} \geq 0$$

for any $k \geq 4$.

Proof of Proposition 2 (*see Appendix A*)

The eigenvector approach associated with the smaller eigenvalue

For mixtures with more than two components, the solution of the system constituted by Eqs. 10 and 11 demands the determination of the vector u, a function of T and P. We will use in the present work the approach proposal by Michelsen (1984), that uses the eigenvector associated with the smaller eigenvalue of second-order tensor $\nabla^2 d(z)$, the Hessian matrix of $d(z)$. Thus, considering a Taylor expansion just as Eq. 7, to minimize q we observed that the smaller value in the quadratic form $q = (1/2)\nabla^2 d(z) \cdot u^2$, with $u \cdot u = 1$, is attained by choosing $u = u_*$ where the unitary vector u_* is an eigenvector associated with the smaller eigenvalue of $\nabla^2 d(z)$. In fact, by Lagrange multipliers theorem [see, for instance, Luenberger (1989)], if $u \in R^{r-1}$ is a minimizer of the problem

$$\begin{cases} \text{Min} & q = \dfrac{1}{2} \nabla^2 d(z) \cdot u^2 \\ \text{s.t.:} & u \cdot u = 1 \end{cases} \tag{13}$$

there exists a single $\lambda \in R$ (Lagrange multiplier) such that $\nabla^2 d(z)u - \lambda u = 0$. Thus, the minimizer of the problem described by Eq. 13 is necessarily an eigenvector of the symmetrical matrix $\nabla^2 d(z)$. After rewriting Eq. 13 in the form

$$q = \frac{1}{2} \nabla^2 d(z) \cdot u^2 = \frac{\lambda}{2} \tag{14}$$

we clearly note that q_* the minimum reached by quadratic form q, occurs when $u = u_*$ that is, the eigenvector associated with the smaller eigenvalue $\lambda_{\min}$, of the matrix $\nabla^2 d(z)$, that is

$$q_* = \frac{1}{2} \nabla^2 d(z) \cdot u_*^2 = \frac{\lambda_{\min}}{2} \tag{15}$$

Therefore, in the critical point (z, T, P), determined u_* the first condition that must occur is $\lambda_{\min} = 0$, or either

$$q_*(z, T, P) = \frac{1}{2} \nabla^2 d(z) \cdot u_*^2 = 0 \tag{16}$$

Consequently, the second condition is

$$c_*(z, T, P) = \frac{1}{6} \nabla^3 d(z) \cdot u_*^3 = 0 \tag{17}$$

Calculation of the quadratic and cubic forms

By deriving Eq. 5 we can calculate the Hessian matrix

$$\nabla^2 d(x) = \left(\frac{\partial^2 d(x)}{\partial x_i \partial x_j} \right)$$

as follows

$$\frac{\partial^2 d(x)}{\partial x_i \partial x_j} = \frac{\partial^2 d(x)}{\partial x_j \partial x_i} = \frac{\partial \mu_i(x)}{\partial x_j} - \frac{\partial \mu_r(x)}{\partial x_j} \tag{18}$$

The chemical potential for each component of the mixture can be written in the following form

$$\mu_i = RT[\ln \phi_i + \ln(Px_i)] + \eta_i(T) \tag{19}$$

where ϕ_i is the fugacity coefficient and $\eta_i(T)$ is an integration parameter that depends only on the temperature and on the nature of the ith component [see Smith et al. (1996)]. Therefore, the calculation of the derivatives of the chemical potential, which appear in the right side of Eq. 18, can be obtained by

$$\frac{\partial \mu_i}{\partial x_j} = RT\left[\frac{\partial \ln \phi_i}{\partial x_j} + \frac{\partial \ln(x_i P)}{\partial x_j} \right] \tag{20}$$

Thus

$$\frac{\partial \mu_i}{\partial x_j} = \begin{cases} RT \dfrac{\partial \ln \phi_i}{\partial x_j} & \text{if } j \neq i \quad \text{and} \quad i \neq r \\ RT\left[\dfrac{\partial \ln \phi_j}{\partial x_j} + \dfrac{1}{x_j} \right] & \text{if } j = i \\ RT\left[\dfrac{\partial \ln \phi_r}{\partial x_j} - \dfrac{1}{x_r} \right] & \text{if } j \neq i \quad \text{and} \quad i = r \end{cases} \tag{21}$$

The fugacity coefficient was calculated using the of Peng–Robinson equation of state with classical mixing rules and the derivatives contained in Eq. 21 are summarized in Appendix B. The binary interaction parameters for the studied systems will be presented in the results section.

With the objective of preventing detailed calculations and elaboration of complicated routines that probably demand appropriate structures of data for its optimized computation, the tensor $\nabla^3 d(z)$, more appropriately the cubic form $c = (1/6)\nabla^3 d(z) \cdot u_*^3$, will be calculated in an approximated manner, as initially suggested by Michelsen (1984). Using the present notation we can approximate, as demonstrated in Appendix C, the cubical form by central differences, as follows

$$c_* = \frac{1}{6} \nabla^3 d(z) \cdot u_*^3 \cong \frac{1}{6\delta^2} [u_*^T \nabla d(z + \delta u_*) + u_*^T \nabla d(z - \delta u_*)] \tag{22}$$

where $\delta > 0$ is a sufficiently small scalar. In all the examples studied here we adopt in Eq. 22 $\delta = 10^{-4}$.

Critical Points Calculation as an Optimization Problem

Formulation of the optimization problem

Considering two intervals ($T_{\min}$, $T_{\max}$) and ($P_{\min}$, $P_{\max}$), where mixture-critical temperature and critical pressure are located, respectively, the calculation of a critical pair (T, P), for each composition z corresponds, by Eqs. 16 and 17, to the solution of the following nonlinear algebraic system

$$\begin{cases} q_*(z, T, P) = \nabla^2 d(z)(T, P) \cdot u_*^2(T, P) = 0 \\ c_*(z, T, P) = \nabla^3 d(z)(T, P) \cdot u_*^3(T, P) = 0 \end{cases} \tag{23}$$

subject to constraints: $T_{\min} < T < T_{\max}$ and $P_{\min} < P < P_{\max}$.

Any iterative procedure used to solve the nonlinear algebraic system described by Eq. 23 demands, at each iteration i, the calculation of $\lambda_{\min}(T_i, P_i)$, the smaller eigenvalue of the matrix $\nabla^2 d(z)(T_i, P_i)$, and $u_*(T_i, P_i)$, the unitary eigenvector associated with $\lambda_{\min}(T_i, P_i)$.

For a specified global composition z, one can consider the nonnegative real function f, which depends on T and P (two variables only), defined as $f(T, P) = q_*^2(z, T, P) + c_*^2(z, T, P)$, with domain $c = (T_{\min}, T_{\max}) \times (P_{\min}, P_{\max}) \subset R^2$, an open box in R^2, where the searched solution is located.

If the system represented by Eq. 23 has a solution, then, to solve this system is equivalent to finding a global minimum of the function $f(T, P)$ inside c.

Thus, the calculation of a critical point can be formulated as the following optimization problem

$$\begin{cases} \text{Min} & f(T, P) = q_*^2(z, T, P) + c_*^2(z, T, P) \\ \text{s.t.:} & T_{\min} < T < T_{\max} \quad \text{and} \quad P_{\min} < P < P_{\max} \end{cases} \tag{24}$$

The formulation of the critical point calculation as an optimization problem offers some advantages: (1) the possibility of using a direct optimization method, which demands only calculations of the objective function f, avoiding calculation (or approximation) of the derivatives of the functions q_* and c_* (these derivatives can be difficult to be obtain); (2) the use of a robust optimization method, which works properly even when the objective function is calculated in an approximated form. For example, the complexity involved in the determination of the third-order tensor $\nabla^3 d(z)$ suggests that the calculation of the cubic form c_* must be conducted by finite differences, which demands and justifies the robustness of the method to be used; (3) the use of an iterative procedure whose convergence is independent on initial guess; and (4) the visualization of the critical phenomenon through the surface and the contour curves of an objective function with only two variables (T and P).

Figure 2 presents typical surfaces and contour curves of objective functions for a mixture containing ethane (component 1), n-pentane (component 2), and n-heptane (component 3), with four different compositions, as presented in Table 1, where T_{c_m} and P_{c_m} represent, respectively, mixture critical temperature and pressure.

In all surfaces contained in Figure 2, the function $f(T, P)$ is defined on the same domain [200 K, 700 K] $\times$ [2000 kPa,

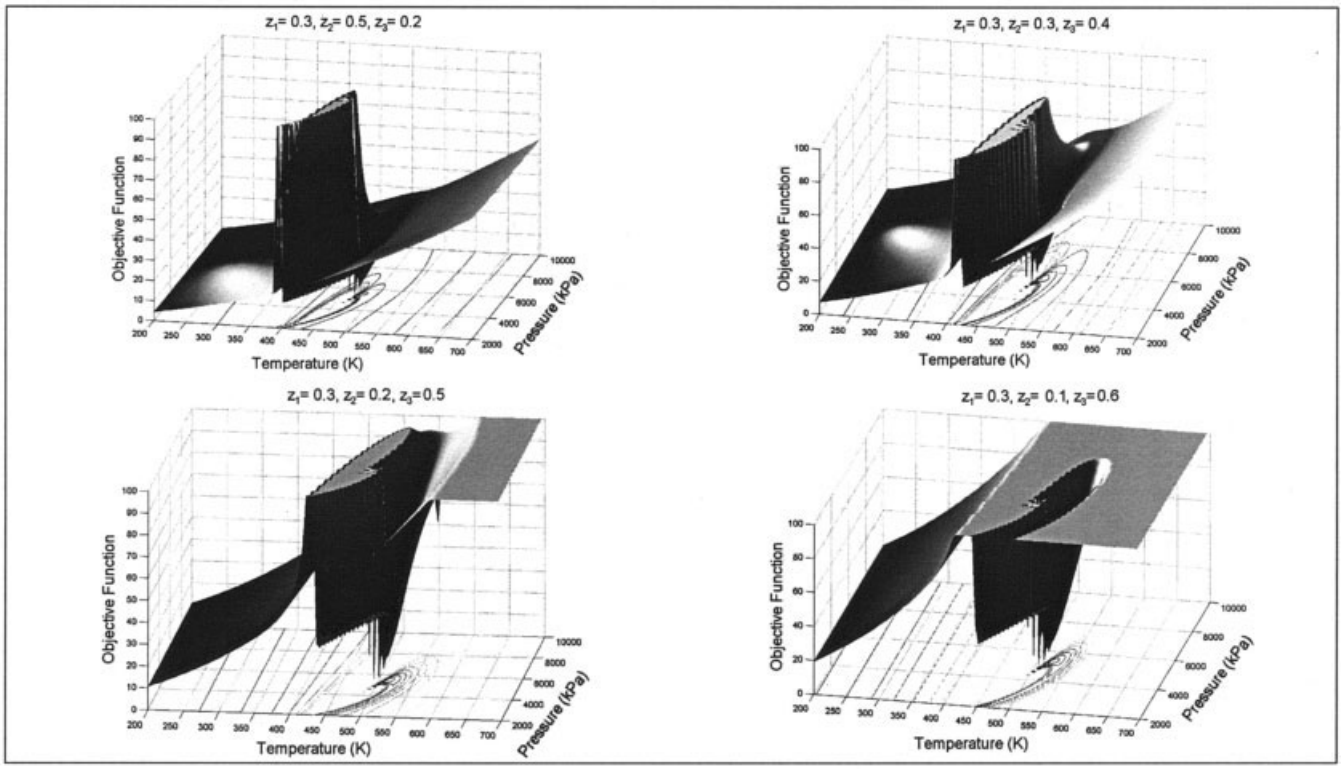

Figure 2. Surfaces of the objective function for the mixture (1) ethane, (2) *n*-pentane, and (3) *n*-heptane with four different compositions.

10,000 kPa]. Observing Figure 2, one can notice that, with exception of the neighborhoods of the critical points, the surface of the objective function presents similar form of many monotonous linear functions (increasing with T). Near critical points, the high nonlinearities of $f(T, P)$ provide sufficient complex geometries. In fact, for values of T and P in the vicinity of the critical point, with lesser temperatures than the critical one, the function assumes relatively high values. As evidenced in Figure 2, the region inside the cardioid curve (or in its neighborhood), described in a T–P plane, refers to the part of the domain with higher values of $f(T, P)$. On this side of this region, the function tends to decrease when T decreases. This part of the feasible domain does not present practical interest for the calculation of critical points, given that any optimization method that uses descent directions, initiating mainly in this region, will tend to converge to the inferior edge of the domain. Even global optimization methods, like the SA algorithm used in the present work, can (when used in not appropriate form, i.e., with an inadequate cooling schedule) converge to the neighborhoods of the inferior boundary of the domain. If it will be convenient, this region can be removed from the feasible domain effectively used in the resolution of the problem described by Eq. 24. We take in all our simulations $T_{\min}$ as being multiple of the pseudocritical temperature of the mixture: $T_{\min} = \alpha \sum_i z_i T_{c_i}$. In a general way, we make $\alpha = 1$; other convenient values for particular cases are presented in the results section. On the other hand, in the vicinity of a critical point, for values of T slightly higher than those related previously, the objective function presents a similar form to an inclined cone with vertex toward low and very fine extremity. As a consequence of these geometric factors, the minimum point (where f is zero) is located in a very narrow valley, where it is difficult to access many optimization methods. Beyond the neighborhood of the critical point, the objective function comes back to grow monotonically with temperature. This last region does not offer difficulty for optimization algorithms.

Table 1. T_{c_m} and P_{c_m} for the Mixture C_2H_6, *n*-C_5H_{12}, and *n*-C_7H_{16}

Composition	$z = (z_1, z_2, z_3)$	T_{c_m} (K)	P_{c_m} (kPa)
1	(0.3, 0.5, 0.2)	469.10	5030.80
2	(0.3, 0.3, 0.4)	499.04	4914.90
3	(0.3, 0.2, 0.5)	489.78	4994.90
4	(0.3, 0.1, 0.6)	507.63	4804.50

The compressibility factor ($Z = Pv/RT$) obtained by a P–v–T model, as used in this work, cannot be unique; that is, the Peng–Robinson cubic polynomial (see definitions of A and B in Appendix B) $Z^3 - (1 - B)Z^2 + (A - 2B - 3B^2)Z - (AB - B^3 - B^2) = 0$ can show one or three real roots. The first surface presented in Figure 2, corresponding to the mixture ethane/*n*-pentane/*n*-heptane, was obtained selecting the largest root (in the case of three real roots). Equivalent surfaces generated using the intermediate root (a) and the smallest one (b) are depicted in Figure 3. It is easy to note that, in spite of the possibility of selecting different surfaces (or, equivalently, different roots), the referred surfaces show that, in the vicinity of the critical point, these graphical forms are identical because the three-root region is far from the critical point. This fact should not be surprising because there is ample evidence in the literature [see, for example, Reid et al. (1988)] that a cubic

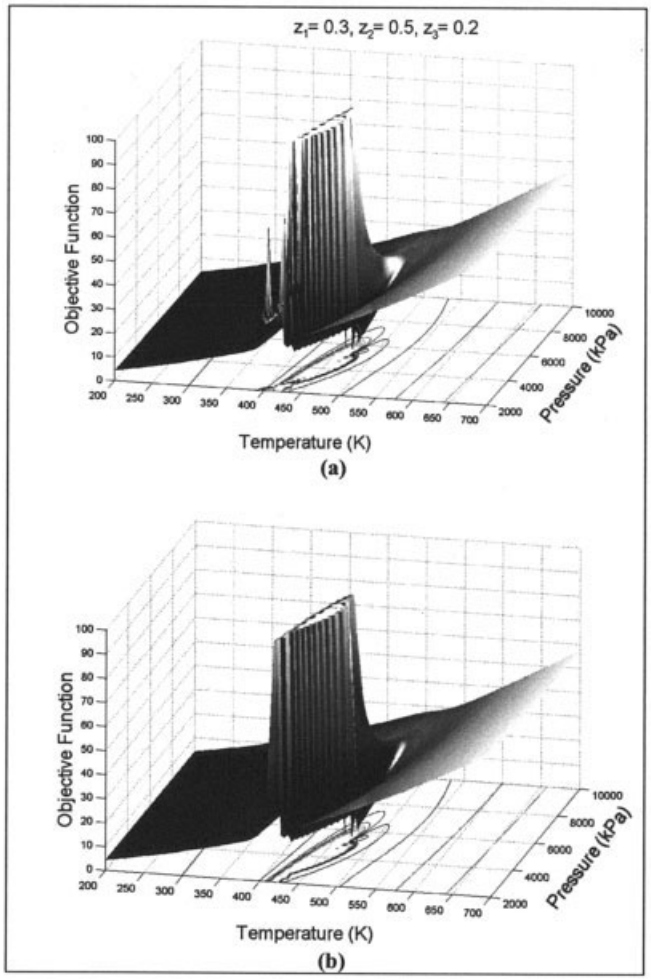

Figure 3. Surfaces of the objective function for the mixture (1) ethane, (2) *n*-pentane, and (3) *n*-heptane evaluated with intermediate (a) and smaller (b) roots.

equation of state has only one real root near the critical region. This argument shows that the choice of the compressibility factor is irrelevant for critical point calculations. In our calculations, we opted for the largest real root.

The simulated annealing algorithm

The geometric complexity of the objective function described previously justifies the use of an appropriate optimization method. Based in our initial experiences (with unsatisfactory results) with classical deterministic methods, we opted to use the SA algorithm. This algorithm has been successfully used in the resolution of several types of phase equilibrium problems [see, for instance, Gomes et al. (2001); Henderson et al. (2001); Pan and Firoozabadi (1998); Zhu and Xu (1999)].

The simulated annealing (SA) algorithm is one of the many heuristic approaches designed to supply points of minimum, not necessarily global, of an objective function within a reasonable time of computation. The SA algorithm presents more search options than those of a descent algorithm. One simple form of a descent algorithm starts with initial guess (called initial solution); then, a point in a neighborhood of this solution is generated by some suitable mechanism and the change in the objective function is calculated. If the generated point promotes a decrease in f, then the current solution is replaced by this new solution; otherwise, the previous solution is retained. The process is repeated until no further improvement in the objective function can be obtained by points in the neighborhood of the current solution. Thus, the descent algorithm terminates at a local minimum. Despite the popularity of this class of algorithms, its disadvantage is in the fact that the point of local minimum found may be, many times, far from the global minimum. One way of improving the solution is to run the descent algorithm several times, starting from different initial solutions and taking the best point found (i.e., that one that produces the lesser value in the objective function).

On the other hand, the SA algorithm can accept steps that lead to an increase in the objective function, and thus is capable of escaping regions of local minimum, searching minimum points in the entire feasible domain. The acceptance of these uphill moves is made in an absolutely controlled way, following probabilistic criteria related to the Boltzmann distribution (see Corana et al., 1987 and Eglese, 1990). The acceptance or rejection of movements, throughout an ascent direction, is determined by the generation of a sequence of random numbers that establish acceptance criteria, from the probabilistic control previously mentioned. The function that supplies the acceptance probability to a movement that causes an increase in the objective function f is called acceptance function and is normally set to $\exp(-\Delta f/\theta)$, where θ is a control parameter, which in an analogy with the physical annealing corresponds to the temperature of the substance. The use of this acceptance function is made in such a way that a movement that produces a small increase in f has a greater probability of being accepted than does a movement that implies a large increase. The function $\exp(-\Delta f/\theta)$ also allows, for high values of θ, many uphill moves to be accepted. However, when θ approaches zero, movements with this property must be rejected. Thus, the SA algorithm initiates with a relatively high value of θ, to prevent its stopping prematurely in the first local minimum found. The SA algorithm carries out a certain number of neighboring changes, at each value of θ, while this parameter is gradually decreased.

The basic steps of the SA algorithm are summarized below (Eglese, 1990), where random(0, 1) represents a random number in the interval (0, 1) and D is the feasible domain of the objective function f.

SA Algorithm

Step 1. Select an initial value x belonging to D.
Step 2. Select an initial control parameter $\theta_0 > 0$.
Step 3. Repeat:
  3a. Repeat initiating from $n = 0$.
    Generate a point y, a neighbor of x.
    Calculate $\Delta f = f(y) - f(x)$.
    If $\Delta f < 0$, then $x = y$.
    Else, if random(0,1) $< \exp(-\Delta f/\theta)$, then $x = y$.
    $n = n + 1$.
  Until $n = N(t)$.
  3b. $t = t + 1$.
  3c. $\theta = \theta(t)$.
Until the stopping criterion is reached.

Table 2. Standard Cooling Schedule

Parameter	Value	Meaning
θ_0	10^3	Initial control parameter
r_θ	0.85	Reduction factor of control parameter
n_θ	15	Maximum number of iterations before reduction of control parameter
n_S	20	Maximum number of cycles

The initial control parameter, the control parameter reduction rate, the number of iterations [$N(t)$] for each value of the control parameter, and the stopping criterion is part of the input data known as cooling schedule. The choice of the cooling schedule is a crucial aspect in the implementation of SA algorithm and can affect the performance of the method. In the present work we use the SA algorithm proposed by Corana et al. (1987). The used cooling schedule is presented in the results section.

Besides the stopping criterion suggested by Corana and coworkers, the quadratic and cubic forms must be sufficiently small. Thus, we accept a pair (T, P) as being a critical point if

$$f(T, P) < \varepsilon_1 \qquad |q_*(T, P)| < \varepsilon_2 \qquad \text{and} \qquad |c_*(T, P)| < \varepsilon_3$$

The tolerances used in all the examples were: $\varepsilon_1 = 10^{-10}$, $\varepsilon_2 = 10^{-5}$, and $\varepsilon_3 = 10^{-5}$.

The SA algorithm presents ease of computational implementation and shows the advantage of being able to deal with optimization problems where the objective function is discontinuous. This last property of the SA is explored, together with other aspects, to supply a methodology used to calculate more than one critical point.

The calculation of the eigenvector associated with the smaller eigenvalue of the Hessian matrix was made using the Jacobi method [see, for instance, Sewell (1990)], a direct method used with symmetrical matrices.

Calculation of more than one critical point

Considering that some mixtures can exhibit various critical points (Stradi et al., 2001), we present a strategy that permits, in these situations, finding more than one critical point. Our approach is relatively simple, although it vigorously explores the calculation of critical points as an optimization problem, solved by the SA algorithm.

We consider initially that, for a given global composition z, a first critical pair denoted by (T_1, P_1) was determined. Then, with the objective of determining a second critical point, we solve (using the SA algorithm) the following problem

$$\begin{cases} \text{Min} & f_1(T, P) = \dfrac{T_{\max} P_{\max}}{|T - T_1||P - P_1|} f(T, P) \\ \text{s.t.:} & T_{\min} < T < T_{\max} \qquad \text{and} \qquad P_{\min} < P < P_{\max} \end{cases} \tag{25}$$

It is clear that near point (T_1, P_1) the function $f_1(T, P)$ becomes arbitrarily high, being discontinuous in this point. Moreover, if the function $f(T, P)$ of Eq. 24 exhibits a second global minimum (T_2, P_2), with $T_2 \neq T_1$ and $P_2 \neq P_1$, then this point also minimizes the function $f_1(T, P)$ given by Eq. 25. Finally, it must be observed that the parameters $T_{\max}$ and $P_{\max}$ are used in the formulation of the function $f_1(T, P)$ to keep the scale of the problem.

In an analogous form, obtained a second critical point (T_2, P_2), if the mixture presents a third critical point, (T_3, P_3), then we determine it by the resolution of the following problem (using the SA algorithm)

$$\begin{cases} \text{Min} & f_2(T, P) = \dfrac{T_{\max}^2 P_{\max}^2}{|T - T_1||P - P_1||T - T_2||P - P_2|} f(T, P) \\ \text{s.t.:} & T_{\min} < T < T_{\max} \qquad \text{and} \qquad P_{\min} < P < P_{\max} \end{cases} \tag{26}$$

If n critical points are already calculated, will look to determine the solution of the $(n + 1)$th critical point, by SA algorithm, for the following minimization problem

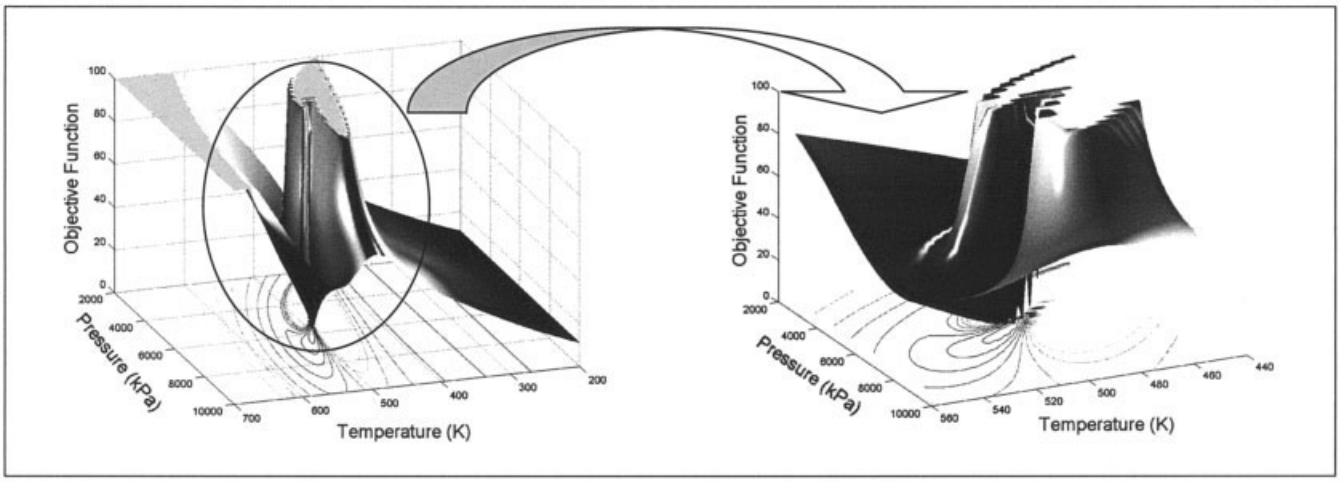

Figure 4. Surface and contour curves of the objective function with amplification of critical region for example 1, with 40% of ethane, 10% of *n*-pentane, and 50% of *n*-heptane.

Table 3. Comparison of Results of This Work and Ekiner and Thodos (1966)

Global Composition	This Work				Ekiner and Thodos (1966)		RD%	
	T_{c_m} (K)	P_{c_m} (kPa)	v (m^3/gmol)	Time (s)	T_{c_m} (K)	P_{c_m} (kPa)	T_{c_m}	P_{c_m}
z = (0.801, 0.064, 0.135)	394.60	8280.30	1.701×10^{-4}	7.25	391.48	8101.00	0.80	2.21
z = (0.615, 0.296, 0.089)	419.30	6926.80	2.112×10^{-4}	6.87	415.92	7060.00	0.81	1.89
z = (0.612, 0.271, 0.117)	424.60	7029.90	2.145×10^{-4}	7.14	421.48	7156.00	0.74	1.76

$$\begin{cases} \text{Min} & f_n(T,P) = \dfrac{T_{\max}^n P_{\max}^n}{\Pi_{i=1}^n |T - T_i||P - P_i|} f(T,P) \\ \text{s.t.:} & T_{\min} < T < T_{\max} \quad \text{and} \quad P_{\min} < P < P_{\max} \end{cases} \tag{27}$$

The presented methodology is easily automatized because the last critical point calculated is removed from the domain, guaranteeing (by SA) that the function does not converge again for this point. The automatization incorporates the visualization of the critical phenomenon only as an auxiliary tool. These are the paradigms of the package Global Critical Simulator (GC-Sim), developed by the *TOG*, at IPRJ-UERJ.

Results and Discussion

In this section we present the computational results and discussions related to application of our methodology for several example problems. In all examples simulated with the SA algorithm developed by Corana et al. (1987), the feasible domain was defined as a closed box in the T–P plane, in the form $[T_{\min}, T_{\max}] \times [P_{\min}, P_{\max}]$, where $T_{\min} = \alpha \sum_i z_i T_{c_i}$ and $P_{\min} = \beta \sum_i z_i P_{c_i}$. Our computational experience with the proposed methodology has indicated the values $\alpha = 1$ and $\beta = 1$ as appropriated to include the critical points in the feasible domain. In the present work, in particular cases where these values are not adequate, other values of α and β are referred to in the text. $T_{\max}$ and $P_{\max}$ are arbitrated sufficiently large, to ensure that the open box $c = (T_{\min}, T_{\max}) \times (P_{\min}, P_{\max})$ contains all critical points searched. We opted by the use of a cooling schedule for the SA algorithm that makes the version of Corana et al. (1987) sufficiently robust. This schedule is presented in Table 2. In spite of the fact of this version of SA algorithm has proved to be insensitive to the initial guess belonging to the feasible domain cited above, in all examples the pair $(T_{\min}, P_{\min})$ has been used as the initial guess. All the examples performed in this work were computed in an AMD Athlon 1.7-GHz processor.

Example 1: three-component system ethane (1), n-pentane (2), and n-heptane (3)

This example presents the results for a mixture of linear alkanes commonly found in oil reservoirs. Critical properties and acentric factor are found in Reid et al. (1988). The binary interaction parameters used are $k_{1,2} = 0.009$, $k_{1,3} = 0.007$, and $k_{2,3} = 0.010$ (Kohse, 1989).

For a global composition z = (0.4, 0.1, 0.5), the mixture presents only one critical point with coordinates $T_{c_m} = 494.07$ K and $P_{c_m} = 5622.80$ kPa. The surface and the contour curves of the objective function are presented in Figure 4. An amplification of the critical region is shown to verify the geometric complexity (as a consequence of the nonlinearities) of the optimization problem. The values of temperature and pressure that define the upper boundary of the feasible domain effectively used in SA algorithm are $T_{\max} = 500$ K and $P_{\max} = 10{,}000$ kPa. The results obtained by SA are fully compatible with the geometric image presented by Figure 4.

To verify the precision of the proposed methodology, we present results for three different compositions, where critical pressures and temperatures are experimentally measured by Ekiner and Thodos (1966). As can be seen from Table 3, the calculated results are very close to the experimental results, with low relative deviations (<1% for critical temperatures and close to 2% for critical pressures). In this table, RD% refers to relative deviation (%). In all cases simulated for this example,

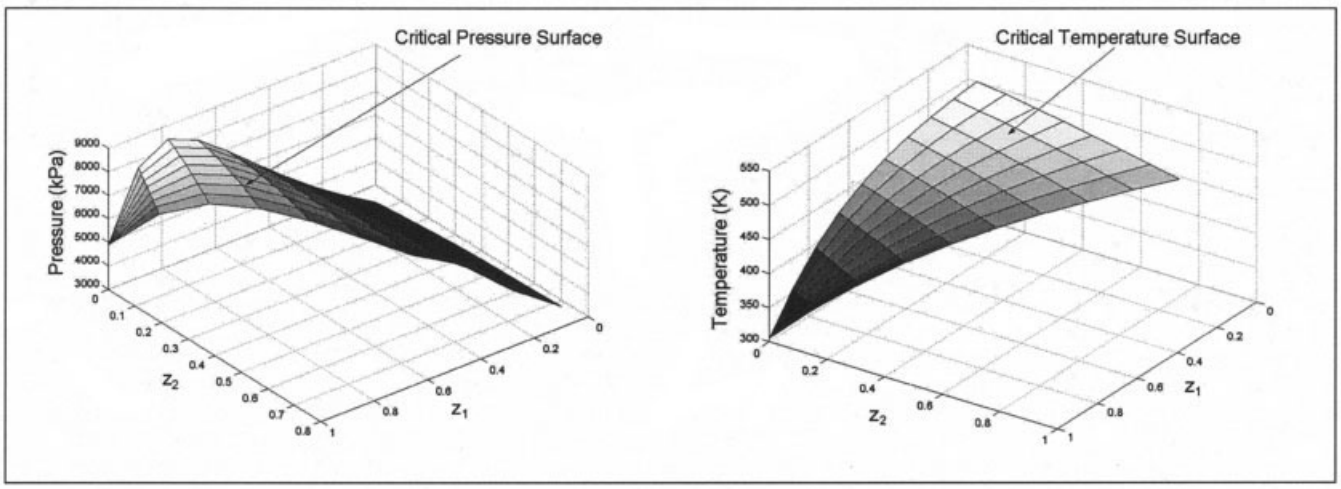

Figure 5. Critical pressure surface and critical temperature surface for example 1.

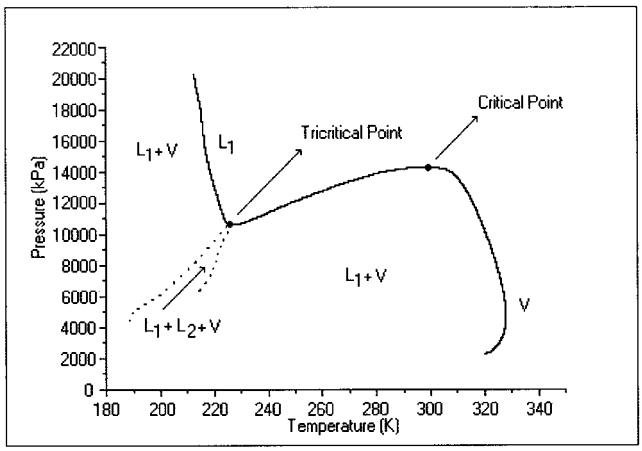

Figure 6. Phase diagram for example 2 with 53.57% of methane, 2.5% of *n*-hexane, and 43.93% of hydrogen sulfide.

one can note that the computational time remains around 7 s (Table 3).

Finally, for the same mixture, to prove the robustness of the proposed methodology, the critical temperature *locus* and the critical pressure *locus* (in the present case, two surfaces) for the entire compositional domain are shown in Figure 5. The compositional domain is described by the molar fractions of ethane and *n*-pentane. Each surface was generated by calculating 80 critical points.

The computational performance of the methodology was also tested for this example. Using a grid with steps equal to 100 K and 1,000 kPa, for initial temperature and pressure, respectively, we generated 40 different initial guesses in the box defined as [100 K, 500 K] $\times$ [3,000 kPa, 10,000 kPa]. The critical coordinates obtained with these initial guesses are virtually the same, the values that are presented in Table 3. The mean elapsed time was 7.17 s, with a standard deviation of 0.03 s. These results show clearly that our methodology does not demand careful initiation strategies, and proves that the computational time remains essentially constant for a given mixture.

Example 2: three-component system methane (1), n-hexane (2), and hydrogen sulfide (3)

In this example a mixture of two hydrocarbons (methane and *n*-hexane) and hydrogen sulfide was studied. This mixture was previously analyzed by Kohse (1989), using a Soave–Redlich–Kwong (SRK) equation of state. This author reported that this mixture, for a specified composition, has two critical points: one of these is classified as a tricritical point involving a triangular region of liquid–liquid–vapor coexistence; the other is an ordinary critical point of a vapor–liquid phase transition. Figure 6 shows the phase diagram for this mixture using Peng–Robinson (PR) equation.

In this example, we used $\alpha = 0.7$, $\beta = 1$, $T_{max} = 700$ K, and $P_{max} = 16{,}000$ kPa. The surface and the contour curves of the objective function for this mixture with a composition $z =$ (0.5357, 0.025, 0.4393) are presented in Figure 7, with an enlargement of the region where the critical phenomenon occurs. This figure clearly indicates the presence of the two critical points described by Kohse and illustrated in Figure 6.

Our methodology, with the suggested cooling schedule (Table 2), was capable of finding the critical points indicated in Figure 7, as demonstrated in Table 4. Although the method proposed here and that used by Kohse use distinct thermodynamic models, the results obtained for both methodologies are very similar. The binary interaction parameters used in the PR equation were $k_{1,2} = 0.040$, $k_{1,3} = 0.080$, and $k_{2,3} = 0.050$ (Kohse, 1989). Again, it is possible to observe that, for a three-component mixture, the computational time is close to 7 s.

Figure 8 exhibits the surface of objective function f_1 (Eq. 25) for two possibilities: the first one uses the tricritical point as T_1 and P_1, whereas in the second possibility the values of T_1 and P_1 correspond to the ordinary critical coordinates. One can note, in the first case, a great discontinuity of f_1 in the neighborhood of the tricritical point (eliminated from the domain of the function f_1). In the second case, as expected, the presence

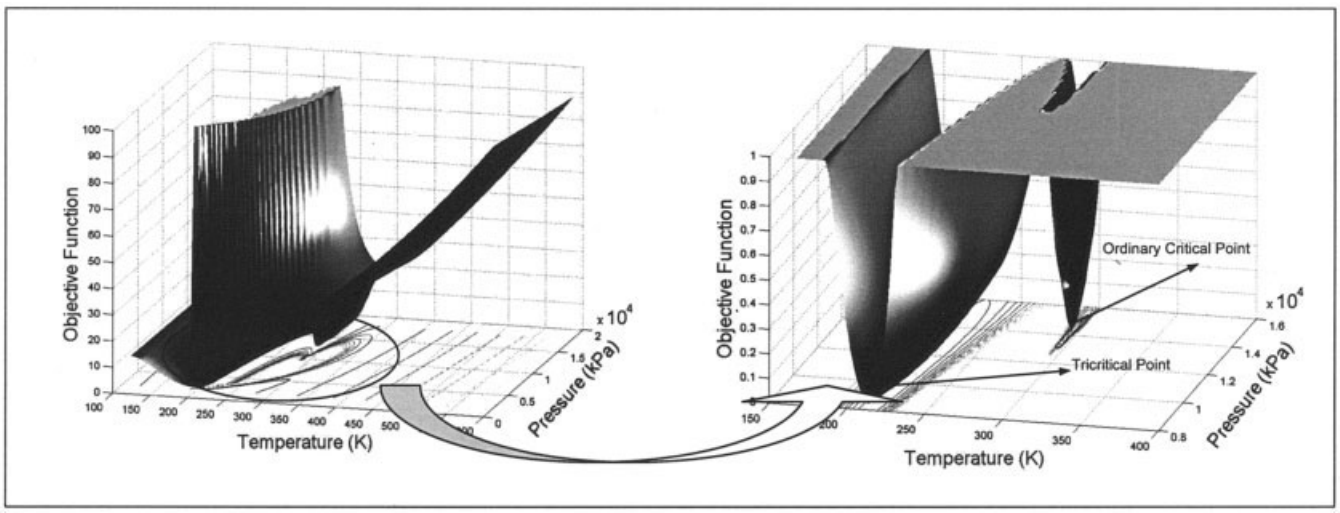

Figure 7. Surface and contour curves of the objective function with amplification of critical region for example 2 with 53.57% of methane, 2.5% of *n*-hexane, and 43.93% of hydrogen sulfide.

Table 4. Comparison of Results of This Work and Kohse (1989)

	This Work (PR)				Kohse (SRK)	
Parameter	T_{c_m} (K)	P_{c_m} (kPa)	ν (m^3/gmol)	Time (s)	T_{c_m} (K)	P_{c_m} (kPa)
Ordinary critical point	295.96	14,178.00	7.166×10^{-5}	7.20	299.40	14,300.00
Tricritical point	219.91	10,767.00	4.354×10^{-5}	6.97	224.40	10,770.00

of the tricritical point is noted, as well as the exclusion of the ordinary critical point.

Example 3: three-component system methane (1), carbon dioxide (2), and hydrogen sulfide (3)

The mixture studied in this example was previously analyzed by Stradi et al. (2001). To illustrate the capability of the SA algorithm to achieve relatively extensive searches in feasible regions, we used, in this case, $\alpha = 0.2$, $\beta = 0.01$, $T_{\max} = 400$ K, and $P_{\max} = 17{,}000$ kPa. The results obtained by Stradi et al. (2001) indicate that this mixture, with a composition of 50% of methane, 10% of carbon dioxide, and 40% of hydrogen sulfide, has two critical points. Table 5 presents the results of our methodology and that found by Stradi et al. (2001). In both works, the binary interaction parameters used were $k_{1,2} = 0.0919$, $k_{1,3} = 0.0$, and $k_{2,3} = 0.0974$.

As can be seen in Table 5, the first critical point found for both methodologies is essentially the same. However, the second calculated point presents a considerable disagreement with respect to the critical pressure. Apparently, the discrepancy indicates a typographical error of these last authors, given that one critical coordinate can be easily obtained using the remaining coordinates, by an equation of state. Table 5 also presents a comparison, only for illustrative purposes (in different machines), of the computation times in the two methodologies, indicating that our approach does not present slow convergence behavior.

Conclusions

In this work we proposed a new formulation for the calculation of critical points as an optimization problem. For this task, a slight modification in the distance function of Gibbs stability test was made. This formulation provides various advantages, among which we cite a very simple strategy for the determination of more than one critical point. When this situation materializes, other critical points can be calculated solving optimization problems strictly related to the original problem, but excluding the critical points previously found. Besides, independently of the number of components, the proposed methodology permits the visualization of the objective function with only two variables (T and P), thus promoting an easy graphical visualization of the critical phenomenon.

The Peng–Robinson cubic equation of state, with classical mixing rules, was used to describe the P–v–T behavior of the thermodynamic systems studied. However, other equations of state and mixing rules can be used without major modifications in the proposed methodology, thus allowing the determination of physically more accurate values for critical temperatures, pressures, and densities.

To solve the proposed optimization problems we used—as an integral part of our numerical procedure—the SA algorithm, a stochastic optimization method that gives preference to global minima and has been currently used in innumerable chemical engineering problems (e.g., Cardoso et al., 1997, 2000; Dolan et al., 1989; Gomes et al., 2001; Henderson et al., 2001). In a similar way with the method proposed by Stradi et al., our strategy allied with the robustness of SA was capable of determining, in all the studied examples, all the existing critical points. Moreover, the convergence of a stochastic optimization method, as used in this work, does not depend on the localization of the initial guess in the feasible domain, and the computational time is approximately constant for mixtures with the same number of components (around 7 s, for three components). On the other hand, nonlinear systems—solved using classical methods such as Newton–Raphson—are sensitive to the localization of the initial guess and to the condition number of the Jacobian matrix. As well known in the literature, the

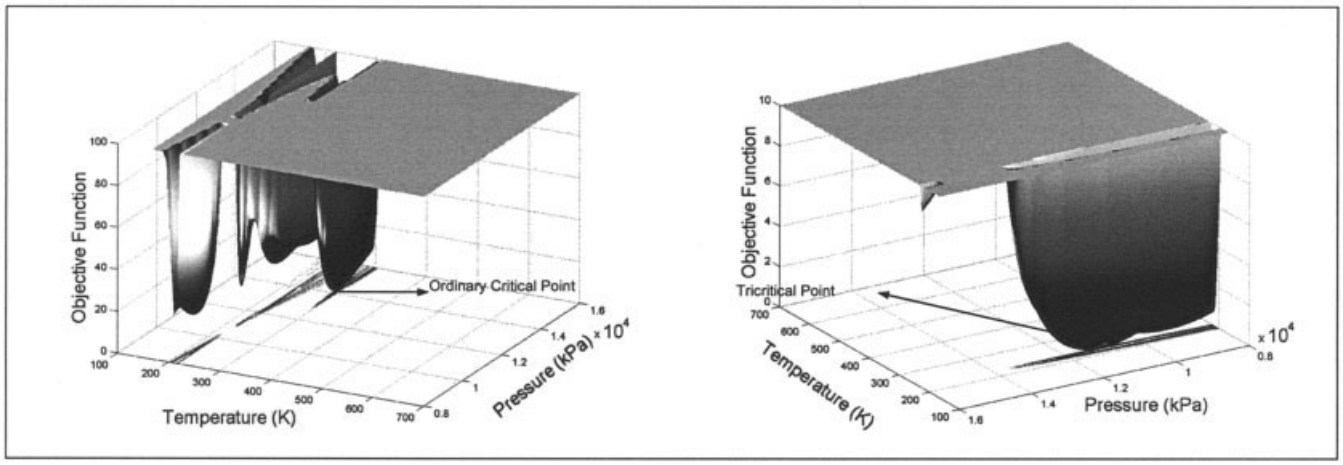

Figure 8. Possible surfaces of the objective function f_1 for the mixture of example 2.

Table 5. Comparison of Results of This Work and Stradi et al. (2001)

	This Work (PR)				Stradi et al. (PR)			
Parameter	T_{c_m} (K)	P_{c_m} (kPa)	ν (m^3/gmol)	Total Time (s)	T_{c_m} (K)	P_{c_m} (kPa)	ν (m^3/gmol)	Total Time (s)
First critical point	285.61	11,376.00	7.236×10^{-5}		285.58	11,380.00	7.235×10^{-5}	
Second critical point	143.48	2957.50	3.223×10^{-5}	14.61	144.36	890.00	3.238×10^{-5}	442

radius of convergence of Newton-type methods is relatively small for many phase equilibrium problems; thus a good initial guess is required before convergence can be achieved (Henderson et al., 2001; Michelsen, 1984). Besides, the use of a direct optimization method as SA avoids the calculation of derivatives of the objective function, thus diminishing the algebraic complexity of the optimization problem and becoming flexible for use with innumerable thermodynamic models, and also for new mixing rules, such as the theoretically correct Wong–Sandler rule (1992) and the Huron and Vidal rule (Huron and Vidal, 1979; Michelsen, 1990). Moreover, the optimization methodology proposed allows the use of the stability criterion developed from other thermodynamic potentials, such as the classical Heidemann and Khalil criterion, that uses the Helmholtz free energy, where T and ν become the primary variables of the problem.

Three types of ternary mixtures were used to test the present methodology. The results of our simulations were compared in a satisfactory way with experimental data, for the first example, and with the other approach, for the second and third examples, illustrating its capability of numerically finding all the critical points in multicomponent mixtures. The graphical visualization of the objective function permitted identification of the existence and localization of the critical points and the tricritical point (the last one for the second example).

Certainly other simulation results are necessary to prove the capability of the proposed methodology to calculate critical points in mixtures that demand a more complex thermodynamic modeling, for instance, mixtures containing strongly polar components such as alcohols, carboxilic acids, and water (Alvarado et al., 1998). In a subsequent report we will present calculations for mixtures involving various critical points.

Literature Cited

Alvarado, G. E., M. Castier, and S. I. Sandler, "Predictions of Critical Behavior Using the Wong–Sandler Mixing Rule," *J. Supercrit. Fluids*, **13**, 49 (1998).

Baker, L. E., A. C. Pierce, and K. D. Luks, "Gibbs Energy Analysis of Phase Equilibria," *Soc. Pet. Eng. J.*, **22**, 731 (1982).

Baker, L. E., and K. D. Luks, "Critical Point and Saturation Pressure Calculations for Multipoint Systems," *Soc. Pet. Eng. J.*, **20**, 15 (1980).

Billingsley, D. S., and S. Lam, "Critical Point Calculation With Non-zero Interaction Parameters," *AIChE J.*, **32**, 1393 (1986).

Callen, H. B., *Thermodynamics and an Introduction to Thermostatistics*, Wiley, New York (1985).

Cardoso, M. F., R. Salcedo, S. Feyo de Azevedo, and D. Barbosa, "A Simulated Annealing Approach to the Solution of MINLP Problems," *Comput. Chem. Eng.*, **21**, 1349 (1997).

Cardoso, M. F., R. Salcedo, S. Feyo de Azevedo, and D. Barbosa, "Optimization of Reactive Distillation Processes with Simulated Annealing," *Chem. Eng. Sci.*, **55**, 5059 (2000).

Corana, A. , M. Marchesi, C. Martini, and S. Ridella, "Minimizing Multimodal Functions of Continuous Variables with the 'Simulated Annealing'Algorithm," *ACM Trans. Math. Software*, **13**, 262 (1987).

Dolan, W. B., P. T. Cummings, and M. D. Le Van, "Process Optimization via Simulated Annealing: Application to Network Design," *AIChE J.*, **35**, 725 (1989).

Eaton, B. E. *On the Calculation of Critical Points by the Method of Heidemann and Khalil*, NBS Technical Note 1313, National Bureau of Standards, Boulder, CO (1988).

Eglese, R. W., "Simulated Annealing: A Tool for Operational Research," *Eur. J. Oper. Res.*, **46**, 271 (1990).

Ekiner, O., and G. Thodos, "Critical Temperatures and Pressures of the Ethane–*n*-Pentane–*n*-Heptane System," *J. Chem. Eng. Data*, **11**, 457 (1966).

Gibbs, J. W., "On the Equilibrium of Heterogeneous Substances" (October 1876–May 1877), *Collected Works*, Vol. 1, Yale Univ. Press, New Haven, CT, p. 55 (1928).

Gomes, J., Henderson, N., and Rocha, M., "Modelling the Vapor–Liquid Equilibrium of Polymer Solutions Using a Cubic Equation of State," *Macromol. Theory Simul.*, **10**, 816 (2001).

Heidemann, R. A., and A. M. Khalil, "The Calculation of Critical Points," *AIChE J.*, **26**, 769 (1980).

Henderson, N., J. R. de Oliveira, Jr., H. P. Amaral Souto, and R. Pitanga Marques, "Modeling and Analysis of the Isothermal Flash Problem and Its Calculation with the Simulated Annealing Algorithm," *Ind. Eng. Chem. Res.*, **40**, 6028 (2001).

Hycks, C. P., and C. L. Young, "The Gas–Liquid Critical Properties of Binary Mixtures," *Chem. Rev.*, **75**, 119 (1975).

Hycks, C. P., and C. L. Young, "Theoretical Predictions of Phase Behaviour at High Temperatures and Pressures for Non-Polar Mixtures: 1. Computer Solution Techniques and Stability Tests," *J. Chem. Soc. Faraday II*, **73**, 597 (1977).

Huron, M. J., and J. Vidal, "New Mixing Rules in Simple Equations of State for Representing Vapor–Liquid Equilibria of Strongly Non-ideal Mixtures," *Fluid Phase Equilib.*, **3**, 255 (1979).

Kohse, B. F., "The Calculation of Tricritical Points," MS Thesis, The University of Calgary, Canada (1989).

Kolář, P., and K. Kojima, "Prediction of Critical Points in Multicomponent Systems Using the PSRK Group Contribution Equation of State," *Fluid Phase Equilib.*, **118**, 175 (1996).

Luenberger D. G., *Linear and Nonlinear Programming*, Addison–Wesley, Reading, MA (1984).

Michelsen, M. L., "Calculation of Phase Envelopes and Critical Points for Multicomponent Mixtures," *Fluid Phase Equilib.*, **4**, 1 (1980).

Michelsen, M. L., "The Isothermal Flash Problem. Part I. Stability," *Fluid Phase Equilib.*, **9**, 1 (1982).

Michelsen, M. L., "Calculation of Critical Points and Phase Boundaries in the Critical Region," *Fluid Phase Equilib.*, **16**, 57 (1984).

Michelsen, M. L., "A Modified Huron–Vidal Mixing Rule for Cubic Equations of State," *Fluid Phase Equilib.*, **60**, 213 (1990).

Michelsen, M. L., and R. A. Heidemann, "Calculation of Critical Points from Cubic Two-Constant Equations of State," *AIChE J.*, **27**, 521 (1981).

Nagarajan, N. R., A. S. Cullik, and A. O. Griewank, "New Strategy for Phase Equilibrium and Critical Point Calculation by Thermodynamic Energy Analysis. Part I—Stability Analysis and Flash," *Fluid Phase Equilib.,* **62**, 191 (1991).

Pan, H., and A. Firoozabadi, "Complex Multiphase Equilibria Calculations by Direct Minimization of Gibbs Free Energy by Use of Simulated Annealing," *SPE Reservoir Eval. Eng.*, **Feb.**, 36 (1998).

Peng, D., and D. B. Robinson, "A New Two-Constant Equation of State," *Ind. Eng. Chem. Fundam.*, **15**, 59 (1976).

Peng, D., and D. B. Robinson, "A Rigorous Method for Predicting the Critical Properties of Multicomponent Systems from an Equation of State," *AIChE J.*, **23**, 137 (1977).

Reid, R. C., and B. L. Beegle, "Critical Point Criteria in Legendre Transform Notation," *AIChE J.*, **23**, 726 (1977).

Reid, R. C., J. M. Prausnitz, and B. E. Poling, *The Properties of Gases and Liquids*, McGraw-Hill, Singapore (1988).
Sadus, R. J., "Calculating Critical Transitions of Fluid Mixtures: Theory vs. Experiment," *AIChE J.*, **40**, 1376 (1994).
Sewell, G., *Computational Methods of Linear Algebra*, Ellis Horwood, London (1990).
Smith, J. M., H. C. Van Ness, and M. M. Abbott, *Introduction to Chemical Engineering Thermodynamics*, McGraw-Hill, New York (1996).
Spear, R. R., R. L. Robinson, Jr., and K.-C. Chao, "Critical States of Ternary Mixtures and Equations of State," *Ind. Eng. Chem. Fundam.*, **10**, 588 (1971).
Stradi, B. A., J. F. Brennecke, J. P. Kohn, and M. A Stadtherr, "Reliable Computation of Mixture Critical Points," *AIChE J.*, **47**, 212 (2001).
Tester, J. W., and M. Modell, *Thermodynamics and Its Applications*, 3rd ed., Prentice Hall, Englewood Cliffs, NJ (1997).
van Konynenburg, P. H., and R. L. Scott, "Critical Lines and Phase Equilibria in Binary van der Waals Mixtures," *Philos. Trans. R. Soc. Lond. A Phys. Sci.*, **298**, 495 (1980).
Zhu, Y., and Z. Xu, "A Reliable Prediction of the Global Phase Stability for Liquid–Liquid Equilibrium Through the Simulated Annealing Algorithm: Application to NRTL and UNIQUAC Equations," *Fluid Phase Equilib.*, **154**, 55 (1999).

Appendix A: Proof of Propositions

Proof of Proposition 1

Differentiating the function $\mu_i = \mu_i(x_1, \ldots, x_{r-1})$ we have

$$d\mu_i = \sum_{j=1}^{r-1} \frac{\partial \mu_i}{\partial x_j} dx_j \tag{A1}$$

By substituting Eq. A1 into the Gibbs–Duhem relation (Eq. 4), we obtain the expression

$$\sum_{j=1}^{r-1} \left(\sum_{i=1}^{r} x_i \frac{\partial \mu_i}{\partial x_j} \right) dx_j = 0 \tag{A2}$$

Because the $r - 1$ molar fractions $x_1, \ldots, x_{r-1}$ are independent variables, then the $r - 1$ differential forms $dx_1, \ldots, dx_{r-1}$ are linearly independent. Thus, from Eq. A2 it follows that

$$\sum_{i=1}^{r} x_i \frac{\partial \mu_i}{\partial x_j} = 0 \qquad \text{for all } j = 1, \ldots, r-1 \tag{A3}$$

On the other hand, deriving the function $d(x)$ with respect to x_j we obtain

$$\frac{\partial d(x)}{\partial x_j} = (\mu_j - \mu_j^0) - (\mu_r - \mu_r^0) + \sum_{i=1}^{r} x_i \frac{\partial \mu_i}{\partial x_j} \tag{A4}$$

By substituting Eq. A3 into Eq. A4 we get Eq. 5 and, therefore, the proposal is proved.

Proof of Proposition 2

Deriving Eq. 5, for $r = 2$, we obtain

$$\frac{\partial^2 d}{\partial x_1^2} = \frac{\partial}{\partial x_1} (\mu_1 - \mu_2) \tag{A5}$$

If n_j represents the number of moles of component $j = 1, 2$, making $n = n_1 + n_2$, one can write $(G/n) = g(x_1, x_2)$, where $G = G(n_1, n_2)$ and $x_j = n_j/n$. Thus, for a binary mixture

$$\frac{\partial g}{\partial x_1} = \frac{1}{n} \frac{\partial G}{\partial x_1} = \frac{1}{n} \left(\frac{\partial G}{\partial n_1} \frac{\partial n_1}{\partial x_1} + \frac{\partial G}{\partial n_2} \frac{\partial n_2}{\partial x_1} \right)$$
$$= \frac{1}{n} \left(n \frac{\partial G}{\partial n_1} - n \frac{\partial G}{\partial n_2} \right) \equiv \mu_1 - \mu_2 \tag{A6}$$

Using Eq. A6 and considering that g is twice differentiable, Eq. A5 can be rewritten as

$$\frac{\partial^2 d}{\partial x_1^2} = \frac{\partial (\mu_1 - \mu_2)}{\partial x_1} = \frac{\partial^2 g}{\partial x_1^2} \tag{A7}$$

Equation A7 demonstrates that $[\partial^2 d(z_1, T, P)]/\partial x_1^2 = 0$ if, and only if, $[\partial^2 g(z_1, T, P)]/\partial x_1^2 = 0$, and, consequently, $[\partial^3 d(z_1, T, P)]/\partial x_1^3 = 0$ if, and only if, $[\partial^3 g(z_1, T, P)]/\partial x_1^3 = 0$. Finally, in a general way, $[\partial^k d(z_1, T, P)]/\partial x_1^k = 0$ if, and only if, $[\partial^k g(z_1, T, P)]/\partial x_1^k = 0$ for all $k \geq 2$; then, a Taylor expansion of d around z_1 (also using Eqs. 2, 5, 10b, and 11b) shows that

$$d(z_1 + h, T, P) = \frac{h^4}{4!} \frac{\partial^4 g(z_1, T, P)}{\partial x_1^4} + \frac{h^5}{5!} \frac{\partial^5 g(z_1, T, P)}{\partial x_1^5} + o(h^6) \geq 0 \tag{A8}$$

for all h such that $0 < z_1 + h < 1$. Therefore, the stability condition described by Eq. A8 is equivalent to affirming that there exists a nonnegative partial derivative of g with order $k \geq 4$, which concludes the demonstration.

Appendix B: Hessian Matrix Calculation of Stability Test Function

In the present work, a and b are obtained by classical mixing rules, as follows

$$a = \sum_{i=1}^{r} \sum_{j=1}^{r} x_i x_j (1 - k_{ij}) (a_i a_j)^{0.5}$$

$$b = \sum_{i=1}^{r} x_i b_i \qquad b_i = 0.077796 \frac{RT_{c_i}}{P_{c_i}} \qquad a_i = a_{c_i} \alpha_i$$

$$a_{c_i} = 0.457235 \frac{(RT_{c_i})^2}{P_{c_i}} \qquad \alpha_i^{0.5} = 1 + m_i \left[1 - \left(\frac{T}{T_{c_i}} \right)^{0.5} \right]$$
$$m_i = 0.37646 + 1.54226\omega_i - 0.26992\omega_i^2$$

where T_{c_i}, P_{c_i}, and ω_i are critical temperature, critical pressure, and acentric factor for pure component i, respectively; and $A = aP/(RT)^2$ and $B = bP/RT$.

$$A = \frac{aP}{(RT)^2} \qquad B = \frac{bP}{RT}$$

To evaluate the partial derivatives $\partial \ln \phi_i/\partial x_j$, using the PR equation of state, the logarithm of fugacity coefficient is written in the following form:

$$\ln \phi_i = \underbrace{\frac{b_i}{b}(Z-1)}_{E_i^{(1)}} - \underbrace{\ln(Z-B)}_{E_i^{(2)}} \underbrace{- \frac{A}{\sqrt{2}aB}\left(\sum_{j=1}^{r} x_j a_{ji}\right)\ln\left(\frac{Z+2.414B}{Z-0.414B}\right)}_{E_i^{(3)}} + \underbrace{\frac{Ab_i}{2\sqrt{2}bB}\ln\left(\frac{Z+2.414B}{Z-0.414B}\right)}_{E_i^{(4)}} \tag{B1}$$

Thus

$$\frac{\partial \ln \phi_i}{\partial x_j} = \frac{\partial E_i^{(1)}}{\partial x_j} + \frac{\partial E_i^{(2)}}{\partial x_j} + \frac{\partial E_i^{(3)}}{\partial x_j} + \frac{\partial E_i^{(4)}}{\partial x_j} \tag{B2}$$

where

$$\frac{\partial E_i^{(1)}}{\partial x_j} = \frac{b_i}{b^2}\left[b\frac{\partial Z}{\partial x_j} - (Z-1)(b_j - b_r)\right] \tag{B3}$$

$$\frac{\partial E_i^{(2)}}{\partial x_j} = \frac{1}{b(B-Z)}\left[b\frac{\partial Z}{\partial x_j} - B(b_j - b_r)\right] \tag{B4}$$

$$\frac{\partial E_i^{(3)}}{\partial x_j} = \frac{1}{\sqrt{2}}\left\{-\frac{A}{aB}\frac{\partial}{\partial x_j}\left[\ln\left(\frac{Z+2.414B}{Z-0.414B}\right)\right]\sum_{k=1}^{r} x_k a_{ki}\right\} + \frac{1}{\sqrt{2}}\left\{-\ln\left(\frac{Z+2.414B}{Z-0.414B}\right)\frac{\partial}{\partial x_j}\left[\frac{A}{aB}\sum_{k=1}^{r} x_k a_{ki}\right]\right\} \tag{B5}$$

$$\frac{\partial E_i^{(4)}}{\partial x_j} = \frac{b_i}{2\sqrt{2}}\left\{\frac{A}{bB}\frac{\partial}{\partial x_j}\left[\ln\left(\frac{Z+2.414B}{Z-0.414B}\right)\right] + \ln\left(\frac{Z+2.414B}{Z-0.414B}\right)\frac{\partial}{\partial x_j}\left(\frac{A}{bB}\right)\right\} \tag{B6}$$

In Eqs. B1–B6, Z is the compressibility factor calculated using PR equation. One can demonstrate that

$$b\frac{\partial Z}{\partial x_j} = \frac{B}{[3Z^2 - 2(1-B)Z] + (A - 2B - 3B^2)} \times \left\{\frac{2(B-Z)}{RT}\sum_{k=1}^{r} x_k(a_{kj} - a_{kr}) + [(A - 2B - 3B^2) + (2 + 6B)Z - Z^2](b_j - b_r)\right\} \tag{B7}$$

Another set of partial derivatives for evaluation of Eqs. B5 and B6 are given by the following expressions:

$$\frac{\partial}{\partial x_j}\left[\frac{A}{aB}\sum_{k=1}^{r} x_k a_{ki}\right] = \frac{A}{aB}\left[(a_{ji} - a_{ri}) - \frac{(b_j - b_r)}{b}\sum_{k=1}^{r} x_k a_{ki}\right] \tag{B8}$$

$$\frac{\partial}{\partial x_j}\left[\ln\left(\frac{Z+2.414B}{Z-0.414B}\right)\right] = \frac{2.828B[-b(\partial Z/\partial x_j) + (b_j - b_r)Z]}{b(Z^2 + 2BZ - 0.999B^2)} \tag{B9}$$

$$\frac{\partial (A/bB)}{\partial x_j} = 2\frac{A}{bB}\left(\frac{\sum_{k=1}^{r} x_k(a_{kj} - a_{kr})}{a} - \frac{(b_j - b_r)}{b}\right) \tag{B10}$$

Appendix C: Approximation of the Cubic Form

Considering that $d(z) = 0$ and $\nabla d(z) = 0$, an expansion of function d in Taylor series around the point z, in the direction of the unitary eigenvector u_* can be written as

$$d(z + su_*) = \frac{1}{2}\lambda_{\min}s^2 + \frac{1}{6}\nabla^3 d(z)\cdot u_*^3 s^3 + \frac{1}{24}\nabla^4 d(z)\cdot u_*^4 s^4 + o(s^5) \tag{C1}$$

By performing differentiation of Eq. C1, we obtain

$$\frac{d}{ds}d(z + su_*) = \lambda_{\min}s + \frac{1}{2}[\nabla^3 d(z)\cdot u_*^3]s^2 + \frac{1}{6}[\nabla^4 d(z)\cdot u_*^4]s^3 + o(s^4) \tag{C2}$$

On the other hand, by the chain rule

$$\frac{d}{ds}d(z + su_*) = \sum_i \frac{\partial d}{\partial x_i}u_* = u^T\nabla d(z + su_*) \tag{C3}$$

By combining Eqs. C2 and C3, we obtain

$$u^T\nabla d(z + su_*) = \lambda_{\min}s + \frac{1}{2}[\nabla^3 d(z)\cdot u_*^3]s^2 + \frac{1}{6}[\nabla^4 d(z)\cdot u_*^4]s^3 + o(s^4) \tag{C4}$$

In an analogous form,

$$u^T\nabla d(z - su_*) = -\lambda_{\min}s + \frac{1}{2}[\nabla^3 d(z)\cdot u_*^3]s^2 - \frac{1}{6}[\nabla^4 d(z)\cdot u_*^4]s^3 + o(s^4) \tag{C5}$$

By adding Eq. C4 to Eq. C5, we have

$$u_*^T\nabla d(z + su_*) = u_*^T\nabla d(z - su_*) = [\nabla^3 d(z) \cdot u_*^3]s^2 + o(s^4) \quad \text{(C6)}$$

Thus

$$c_* = \frac{1}{6}\nabla^3 d(z) \cdot u_*^3 = \frac{1}{6s^2}[u_*^T\nabla d(z + su_*) + u_*^T\nabla d(z - su_*)] + o(s^2) \quad \text{(C7)}$$

If we get $s = \delta$, where $\delta > 0$ is a scalar sufficiently small, the cubic form can be approximated with an error of order $o(\delta^2)$ by the following scheme of central differences:

$$c_* = \frac{1}{6}\nabla^3 d(z) \cdot u_*^3 \cong \frac{1}{6\delta^2}[u_*^T\nabla d(z + \delta u_*) + u_*^T\nabla d(z - \delta u_*)] \quad \text{(C8)}$$

Manuscript received May 13, 2003, revision received July 18, 2003, and final revision received Oct. 8, 2003.